

Cite this: *Nanoscale*, 2019, **11**, 22196

# High-performance sodium-ion batteries with a hard carbon anode: transition from the half-cell to full-cell perspective

 Xinlong Chen,<sup>†a,b</sup> Yuheng Zheng,<sup>†a,b</sup> Wenjian Liu,<sup>a,b</sup> Can Zhang,<sup>a,b</sup> Sa Li<sup>\*a,b</sup> and Ju Li<sup>ID \*c</sup>

Hard carbon is an appealing anode material for sodium-ion batteries (SIBs) due to renewable resources, low cost and high specific capacity. Practical full cells based on hard carbon with high energy density and long cyclability are expected to possess application interest for grid-scale energy storage. In this review, following this archetypal use scenario of SIBs, we aim at providing a quantitative full-cell metric for evaluating newly designed anodes or cathodes. Some significant problems in conventional half-cell and full-cell tests, including unfaithful prediction of capacity loss by coulombic efficiency in the full-cell and under-estimated capacity of hard carbon in the half-cell test, are discussed to better assess the actual capacity and cyclability of the hard carbon anode in sodium-matched full cells. Finally, we review rational design of hard carbon itself and the selection of electrolytes from such a full-cell perspective.

Received 1st September 2019,

Accepted 14th October 2019

DOI: 10.1039/c9nr07545c

rsc.li/nanoscale

## 1. Introduction

With increasing research investment in sodium-ion batteries (SIBs), they have gradually come into maturity and entered the arena competing with lithium-ion batteries (LIBs).<sup>1</sup> Hard carbon possesses many advantages,<sup>1–4</sup> such as high initial coulombic efficiency (ICE),<sup>1</sup> decent gravimetric specific capacity (roughly more than 2× that of well-known cathodes such as layered oxides<sup>5</sup> and polyanionic compounds<sup>2,6,7</sup>), as well as stable cycling capacity,<sup>4</sup> and thus is regarded as a star class of anode materials for SIBs. The reported evaluated energy density of the SIB full-cell with hard carbon anode could approach 200 W h kg<sup>−1</sup>, which comes near to the commercialized graphite//LiFePO<sub>4</sub> based LIBs,<sup>8,9</sup> and the raw material cost would not get higher than that of LIBs.<sup>10</sup> Moreover, the much more abundant and evenly distributed sodium and carbon resources could remove the possibility of geopolitical supply crises, which have already occurred for Lithium. Encouragingly, some significant advancements in the full-cell assembly have been made.<sup>1,8,9</sup> Zheng *et al.*<sup>1</sup> obtained a very competitive sodium-matched full-cell based on the hard carbon anode, which delivered a high

energy density of 186 W h kg<sup>−1</sup> at 1 C and a capacity retention of 70% after 1300 cycles. Even at a high rate of 5 C, a full-cell with hard carbon can still deliver a long cyclability of 1200 cycles.<sup>8</sup> However, surprisingly, when employing the conventional half-cell testing metric, hard carbon sometimes failed to impress.<sup>1,11</sup> It was later revealed that in half cells, the sodium metal counter-electrode incurs large impedance, which often leads to an overly pessimistic indication of half-cell performance, underutilizing the low-lying plateau part of hard carbon's capacity.

It is important to point out that hard carbon is not a specific material, but a class of carbonaceous materials with a quite wide variation in micro-structures and consequently different electrochemical behaviors in SIBs.<sup>9,12</sup> The term “hard” in hard carbon points to its mechanically harder characteristic than graphite or “soft carbon”, which can deform more easily by interplanar sliding. Hard carbon cannot be turned to crystalline graphite upon simple heating in a reducing atmosphere, whereas soft carbon can. The structural model of hard carbon will be further discussed at the end of this review, but it is generally believed to have higher orientational disorder and porosity between its sp<sup>2</sup>-nanodomains, and such disorder and porosity are locked in so strongly that they can be maintained even up to 3000 °C, without complete graphitization. Soft carbon also has sp<sup>2</sup>-nanodomains and disorder in between, but in contrast, it is more compact due to the higher content of hydrogen in the precursors which makes the carbon atoms more mobile at the earlier stage of carbonization, such that the orientational disorder between the nanodomains is not locked in so strongly that they can be elimi-

<sup>a</sup>School of Materials Science and Engineering, Tongji University, Shanghai 201804, China. E-mail: lisa@tongji.edu.cn

<sup>b</sup>Institute of New Energy for Vehicles, Tongji University, Shanghai 201804, China

<sup>c</sup>Department of Nuclear Science and Engineering and Department of Materials Science and Engineering, Massachusetts Institute of Technology, Cambridge, MA 02139, USA. E-mail: liju@mit.edu

<sup>†</sup>The authors contribute equally to the article.



nated and can finally coarsen to large graphite crystals around 3000 °C.<sup>13</sup> Practically speaking, one can distinguish “hard carbon” and “soft carbon” components according to the real density and low-angle XRD patterns.<sup>13</sup> Note that some hard carbon could also be graphitized under high pressure<sup>14</sup> or with catalysts,<sup>15,16</sup> and the anthracite-derived hard carbon at 1600 °C could even lose its porosity through further heating between 2000 °C and 2500 °C and turns “soft”, transforming from non-graphitizing carbon to graphitizing carbon.<sup>13</sup> It is clear from the above discussion that hard carbon does not have a black-and-white definition, similar to the “microcrystal-nanocrystal-glass” continuum in metallurgical definitions. Indeed, when one produces a carbonaceous electrode material by heating, say some biological matter to 1200 °C in a reducing atmosphere, the resulting product could be a heterogeneous mixture of hard carbon and soft carbon. In this review, as long as the mechanically hard, lower-density and “non-graphitizable” component is the majority, we will accept such a heterogeneous mixture as “hard carbon”.

Due to the complexity of the structure/electrochemical behaviors and the vulnerable half-cell performance of hard carbon as mentioned above, it is conceivable that some high-performance hard carbon anodes might have once been synthesized but the overly pessimistic indication of half-cell results might have prevented a further full-cell evaluation. Hence, in this review, we first provide a discussion of the full-cell evaluation perspective, to figure out what is essential for one specific anode material when applied to SIBs. Then the reason for the pessimistic indication of half-cell results is revealed and a revised half-cell test (RHT) method is introduced to provide a useful reference capacity (but not cycle life) before designing the full-cell match-up. Finally, based on this full cell perspective, we review rational design of the hard carbon material and electrolyte selection.

## 2. Developing promising full-cell metrics of SIBs

While tremendous effort has been spent on SIB research, it is frustrating that actually not as many researchers pay attention to the full-cell perspective. A full cell requires pairing an anode with a real cathode such as O<sub>3</sub>-Na<sub>0.90</sub>[Cu<sub>0.22</sub>Fe<sub>0.30</sub>Mn<sub>0.48</sub>]O<sub>2</sub><sup>17</sup> or Na<sub>3</sub>V<sub>2</sub>(PO<sub>4</sub>)<sub>2</sub>F<sub>3</sub><sup>18</sup> with roughly balanced areal capacities and limited Na inventory, not superabundant sodium metal. The areal capacities have the unit of mA h cm<sup>-2</sup>, and for industrial applications, they are typically above 2 mA h cm<sup>-2</sup>. Specifically, the areal capacities of the cathode and anode must be matched based on the half-cell nameplate specific capacities and initial coulombic efficiency (ICE), with a little capacity redundancy on the anode side (5%–10% in the LIB industry) to avoid local sodium–metal deposition caused by heterogeneous current density. Some materials researchers may complain about the availability of appropriate SIB cathodes with matching areal capacity and the complexities of designing a well-matched full-cell battery and stop their research at the

level of half-cells against a Na<sub>BCC</sub> counter electrode with extremely large cyclable Na inventory (10× or even 100× in excess). However, the presence of a superabundant Na<sub>BCC</sub> metal chip counter electrode with a lot of electrolyte can hide potential problems of the material being tested, which will show up in an unpleasant way when finally adopted in practical full cells (“overly optimistic” half-cell prediction). Na<sub>BCC</sub> is also highly reactive with liquid electrolytes (much more so than Li<sub>BCC</sub>) and the resultant large polarization on voltage<sup>11</sup> will result in the undervalued capacity of hard carbon anode as discussed in Sec. 3 and might also bury some gold in bricks (“overly pessimistic” half-cell prediction) in the materials selection stage.

Currently, many researchers focus on improving the gravimetric energy density ( $E_g$ ) or the volumetric energy density ( $E_v$ )<sup>19</sup> of SIBs. But it is unadvisable to ignore the detailed price modeling aspect and take for granted that all the SIBs are cheaper than LIBs. A useful full-cell metric should fully consider its application scenario, and a crude  $p$  metric to estimate the economic competitiveness of a SIB full-cell is

$$p = C/(E \cdot L), \quad (1)$$

where  $C$ ,  $E$ , and  $L$  represent the total cost (unit \$), discharge energy (unit kW h) per cycle, and cycle life of the battery (defined as dropping to 80% of the initial discharge energy), respectively. To improve the  $p$  value, researchers should pay attention to lowering the total cost per kW h of full-cell batteries and developing SIBs with a longer cycle life. The total cost is calculated by adding all the expenses of raw materials and processing and financing costs, and the total energy could be calculated by multiplying capacity and the average of full-cell voltage  $V \equiv U_{\text{cathode}} - U_{\text{anode}}$ .<sup>10</sup> Since the cycle life  $L$  can be a highly nonlinear function of the depth of discharge (DOD),<sup>20,21</sup> which affects  $E$ , the optimization of  $p$  as well as the down payment (CAPEX)  $C/E$  may lead to an optimal solution with the DOD significantly less than 1. This in turn means that the anode and cathode may be operated in restricted voltage/capacity regimes that do not span the full range, respectively. The full-cell voltage cutoffs [ $V_{\text{lower}}$ ,  $V_{\text{upper}}$ ] in charging and discharging are also design parameters that affect  $E$  and  $L$  and may be optimized to improve  $p$  and  $C/E$  together.

CE is an important figure-of-merit since the coulombic inefficiency (CI  $\equiv 1 - \text{CE}$ ) is believed to be an accurate reflection of how much lithium or sodium inventory is irreversibly consumed in one cycle, and it is commonly understood that CE should exceed 99.9% to achieve 200 cycles since  $0.999^{200} = 0.8186$ . Currently, few commercial battery cyclers are actually qualified for such a high-precision measurement.<sup>22</sup> Besides, even if CE can be recorded without any error, CI may still be overly pessimistic in evaluating how quickly the cyclable alkali ions are trapped and turn non-cyclable. As one cannot directly follow and count ions moving inside the cell and can only count electrons moving in the outer circuit, one have to infer what happens inside the cell based on some assumptions about what can and cannot move in the electrolyte and what can or cannot be accepted/generated at the electrolyte/elec-



trode interfaces. CE is detected technically in the outer electronic circuit as the ratio of the electronic discharge capacity ( $Q_{ed}$ ) to charge capacity ( $Q_{ec}$ ) in one cycle, and they are not necessarily equal to the ionic discharge capacity ( $Q_{id}$ ) and charge capacity ( $Q_{ic}$ ) inside the cell.<sup>23</sup> Actually, due to some soluble redox mediators,<sup>8,23</sup> the electrolyte may gain some electronic conductivity, resulting in a “leaking” electronic current from the anode to the cathode side continuously which leads to a leaked capacity in discharge ( $Q_{id}$ ) and charge ( $Q_{ic}$ ), respectively. Thus, there will always be

$$CE \equiv Q_{ed}/Q_{ec} = (Q_{id} - Q_{ld})/(Q_{ic} + Q_{lc}) < Q_{id}/Q_{ic} \quad (2)$$

and  $CI > (Q_{ic} - Q_{ld})/Q_{ic}$ . For example,  $CO_2$  solvated in the liquid electrolyte could cause a shuttling or self-discharge effect in LIBs.<sup>24</sup> In our previous report on a sodium-ion full-cell which exhibits a much greater shuttling effect than LIBs, the cycle life is  $\sim 5\times$  better than what the CI cumulant prediction suggested based on half-cell characterization of the hard carbon electrode.<sup>8</sup> Thus, the cycle life of SIBs ( $L$ ) should be carefully verified from the real cycling of the well-balanced full-cell battery, rather than relying on CE prediction alone.

### 3. Revealing the undervalued half-cell test results

To achieve a lower  $p$  of eqn (1), the cathode and anode should be well matched in areal capacities to avoid the unnecessary redundancy of the electrode mass, increasing  $E$  and reducing  $C$ . The areal capacities are usually estimated from traditional half-cell tests (THTs), on the anode and on the cathode separately. (We have already mentioned that THT can be an overly pessimistic indicator of cycle life, but here we are just talking about first-10-cycle capacity.) But surprisingly, when running THT with voltage cutoffs  $[V_{lower}, V_{upper}] = [0 \text{ V}, 2.0 \text{ V}]$ , it was found that such THT first-10-cycle capacity is still not qualified for quantifying the true reversible areal capacity of hard carbon. The reason turns out to be due to overpotential in dynamic charging, especially coming from that of the  $Na_{BCC}$  counter-electrode in a two-electrode cell setup.

#### 3.1. Why the areal capacity of hard carbon can be largely underestimated in THT

It seems natural that the half-cell ought to perform better than the areal capacity-matched full-cell in cyclability and capacity, since the counter electrode  $Na_{BCC}$  metal provides almost endless Na inventory, which is expected to be consumed continuously at the anode/electrolyte interface for parasitic reactions. But actually it was reported<sup>1</sup> that in a traditional half-cell test, the sodium-matched full-cell based on the hard carbon anode could survive for 1300 cycles at 1C with a capacity retention of 70%, while the sodium-metal redundant half-cell possessed only  $\sim 1/6$  of the capacity delivered in the full-cell and appeared to have died within 100 cycles at the same current density.

The key to understanding the apparent capacity difference between the half and full-cell is the different triggering regimes of voltage truncation in sodiation of hard carbon and how sensitive they are with respect to the current density  $\dot{Q}$  in dynamic charging tests. The THT 0 V cutoff, a convenient and often-taken operational measure, often corresponds to the plateau part of the open-circuit voltage (OCV) profile of hard carbon  $U_{anode}^{OCV}(Q)$ , where  $Q$  is the areal capacity and the subscript “anode” here just stands for hard carbon. How this truncation is actually triggered is shockingly sensitive to the current density  $\dot{Q}$ :  $U_{anode}(\dot{Q}, Q) \neq U_{anode}^{OCV}(Q)$ ,  $U_{NaBCC}(\dot{Q}, Q) \neq U_{NaBCC}^{OCV}(Q) \equiv 0$ . In other words, one can easily prematurely truncate in the THT test when  $V^{THT} \equiv U_{anode} - U_{NaBCC}$  hits zero, due to  $U_{anode}(\dot{Q}, Q) < U_{anode}^{OCV}(Q)$  and  $U_{NaBCC}(\dot{Q}, Q) > U_{NaBCC}^{OCV}(Q) \equiv 0$  during the sodiation process of hard carbon, even when  $U_{anode}^{OCV}(Q)$  is above zero and physically in a reversible regime of the hard carbon capacity. In contrast, since full-cell voltage  $V \equiv U_{cathode} - U_{anode}$ , and  $U_{cathode}^{OCV}$  maintains a significant slope with respect to  $Q$ , the sodiation process of hard carbon is likely truncated at a sloping part of full-cell  $V^{OCV}(Q)$  in charging, which is much more tolerant to polarization, as shown in Fig. 1(A and B).<sup>1</sup> Premature truncation due to high  $\dot{Q}$  tends not to occur in the full-cell test since we rely more on  $U_{cathode} \uparrow$  to trigger the full-cell voltage cutoff, if we design the anode to be slightly capacity-excess than the cathode (of course, this relies on knowing what the reversible capacity of the anode roughly is beforehand, so this is a chicken-and-egg iterative problem, if we do not have a reliable half-cell test protocol). Note that the OCV curve is very time-consuming to measure, while in standard battery cycling tests, the current density is so high that significant polarizations (deviation of  $U_{cathode}$  from  $U_{cathode}^{OCV}$  and  $U_{anode}$  from  $U_{anode}^{OCV}$ ) can arise. Ji's group<sup>11</sup> further confirmed this phenomenon using the three-electrode testing method and the results are shown in Fig. 1(C). Due to polarization, the cutoff of 0 V in  $V \equiv U_{hard\ carbon} - U_{NaBCC}$  in THT will indeed result in the premature ending of “plateau part” of  $U_{hard\ carbon}^{OCV}$  (even though the open-circuit voltage is still above 0 V versus  $Na^+/Na_{BCC}$  and also  $Na_{BCC}$  does not actually precipitate out in these THT half-cell tests) and it gets much more obvious at a higher current density, which leads to the undervalued rate capacity of hard carbon. In some cases, for example when the battery is tested at a low current density, the effect of polarization may not be severe enough in THT and many researchers indeed obtain high-capacity hard carbon anodes, but the capacity could still be somewhat underestimated as discussed above. It is also worth mentioning that electrochemical polarization on the superabundant  $Na_{BCC}$  counter-electrode, which leads to the undervalued half-cell results, is not just specific to SIBs, but is a common issue in all alkali ion batteries. The only difference might lie in the degree of impact, and actually the  $Na_{BCC}$  metal is more severe than the  $Li_{BCC}$  metal<sup>25</sup> as shown in Fig. 1(D). Larger electrochemical polarization of SIB half-cells results from the higher parasitic reactions of the Na metal with the liquid electrolyte, which introduces larger impedance related to the SEI layer,<sup>25,26</sup> compared to LIB half-cells. For the time being, this



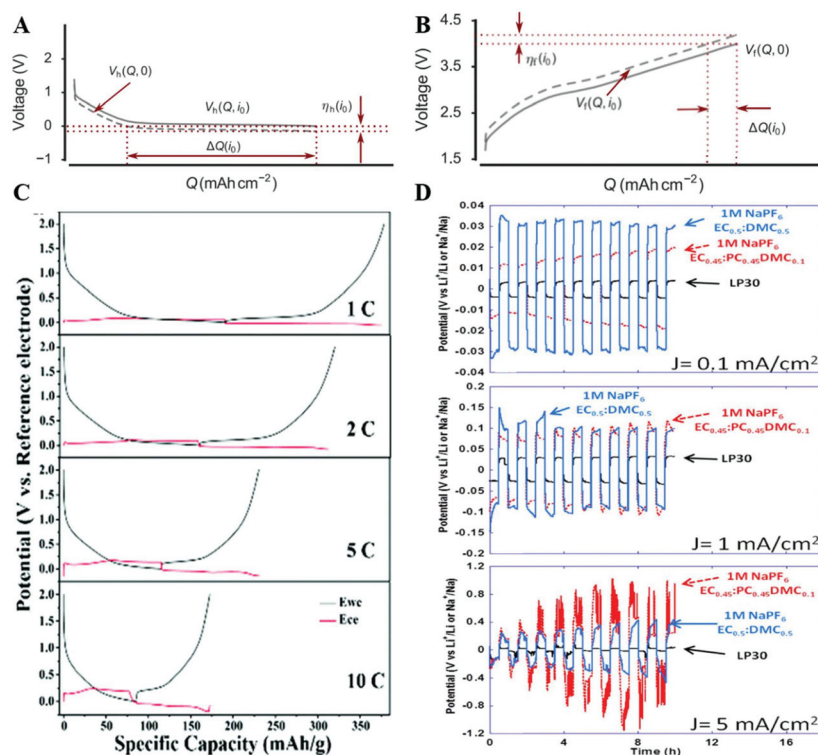


**Fig. 1** (A and B) The influence of cell polarization on the half-cell and full-cell, respectively.<sup>1</sup> Reproduced with permission from ref. 1. Copyright 2017. Elsevier. (C) Sodiation–desodiation potential profiles of FP-HC of the fifth cycle at different current rates in the three-electrode cell, which clearly presents the influence of polarization, where  $E_{we}$  represents the working electrode and  $E_{ce}$  represents the counter electrode of the Na metal.<sup>11</sup> Reproduced with permission from ref. 11. Copyright 2017. The Royal Society of Chemistry. (D) The influence of different electrolytes on the degree of electrochemical polarization in both LIBs and SIBs.<sup>25</sup> Reproduced with permission from ref. 25. Copyright 2015. ECS-The Electrochemical Society.

difference is difficult to resolve systematically due to the extreme reactivity of sodium metal and the absence of reliable Na foil.<sup>26</sup> Meanwhile, due to the much more severe reaction between Na<sub>BCC</sub> metal and electrolyte, the SIB half-cell may die quickly due to electrolyte dryout, causing a much shorter cycle life. Thus, we highly recommend that the researchers should take polarization and electrolyte consumption into consideration and think twice about the THT half-cell test of other alkali ion batteries based on rigid voltage cutoffs [ $V_{lower}$ ,  $V_{upper}$ ] like [0 V, 2.0 V], due to excessive polarization on Na<sub>BCC</sub> even at quite small current densities.

### 3.2. A revised half-cell test (RHT) method

Traditionally, the THT half-cell test is an essential step to examine the specific capacity, rate performance and cyclability of a newly designed electrode material. However, without using the Na<sub>BCC</sub> metal anode, the capacity-balanced full-cell with a transition-metal-oxide cathode and a hard carbon anode can actually exhibit much better specific capacity, rate capability and cycle life as discussed previously.<sup>1</sup> Thus, we strongly advise that more attention should be paid to the sodium-matched full-cell.

However, it is still a very inconvenient and iterative construction-testing process to directly work with full cells. Before designing a sodium-matched full-cell, some kind of half-cell

test is still needed to ascertain and quantify the specific capacity and ICE as mentioned before, and hence a revised half-cell test (RHT) method which can precisely locate the true capacity and ICE is developed. We recommend RHT to be used to assess the initial capacity and ICE, before designing the sodium-matched full-cell, to save time and cost. But the cycle life of hard carbon should still be better assessed by the full-cell test, not with THT or RHT.

Considering that in practical usage scenarios, all the capacity before nucleation of Na<sub>BCC</sub> on the surface of hard carbon is actually acceptable, we define reversible anode capacity as the maximum capacity right before nucleation of Na<sub>BCC</sub> at a certain current density/rate and cathode capacity could be defined as the capacity within a certain voltage range at a certain current density/rate. A three-electrode setup might be an acceptable scheme<sup>11</sup> to remedy the effect of polarization on the Na-metal counter electrode, but is more complicated to conduct.

Zheng *et al.*<sup>1</sup> provided a revised half-cell test (RHT) method, in which the initial cycle of THT is reserved to get the ICE, and in the second cycle, the discharging cutoff voltage of 0 V is removed and more attention is paid to the nucleation signature in the voltage that will fall below 0 V. As shown in Fig. 2(A and B), there is a “V”-shaped voltage cusp between the highly reversible parts and BCC metal deposition part in both LIBs





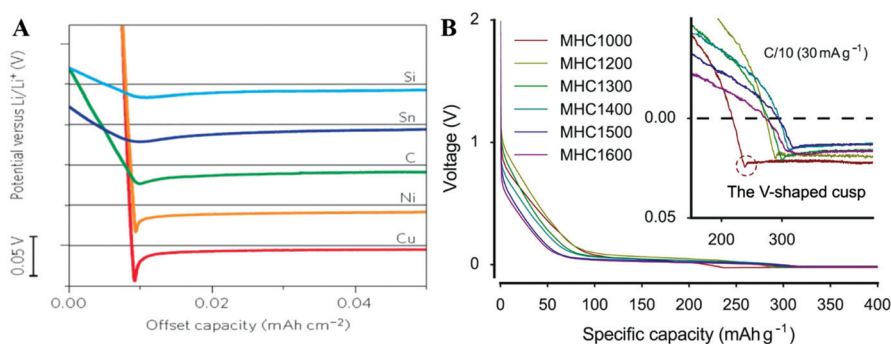


**Fig. 2** (A) Voltage profiles during Li deposition on various materials which show the appearance of the V-shaped cusp.<sup>27</sup> Reproduced with permission from ref. 27, Copyright 2016. Springer Nature. (B) The V-shaped cusp in the hard carbon half-cell.<sup>1</sup> Reproduced with permission from ref. 1. Copyright 2017. Elsevier.

and SIBs, caused by the nucleation energy barrier<sup>27</sup> of the body-centered cubic (BCC) Li/Na metal. This V-shaped cusp indicates the end of reversible capacity precisely even if the half-cell voltage is a little negative. In their work, the half-cell delivers a specific capacity of  $314 \text{ mA h g}^{-1}$  in RHT, which is in excellent agreement with the full-cell test in long-term cycling. Thus, RHT first-cycle capacity provides a good estimate for designing a full cell, which requires  $\sim 5\%$  overcapacity on the hard carbon side compared to the cathode side, which is sufficient to prevent  $\text{Na}_{\text{BCC}}$  nucleation on the hard carbon surface.

## 4. Research outlook: sodium storage mechanism and developing high-performance SIBs with hard carbon

Based on the full-cell evaluation metric, high-performance SIBs should possess the advantages of low cost per kW h and a long cycle life. High specific capacity (low  $C/E$ ) and high CE (long  $L$ ) are essential for hard carbon to reduce the cost of the full-cell according to the model.<sup>10</sup> The cycling capability of hard carbon is acceptable since the sodium-matched full-cells could survive for more than 1000 cycles.<sup>1,8</sup> However, due to the lack of explicit knowledge of the sodium storage mechanism, it becomes quite a tough mission to carry out rational design of the hard carbon material. Most of the material explorations so far are processing followed by testing. Herein, we will first review the historical understanding of the sodium storage mechanism in hard carbon. Several more systematic attempts, including using various precursors, amending the pyrolysis process and doping heteroatoms, will also be discussed. Lastly, since the electrolyte plays a critical role in  $p$ , as the amount and stability of SEI formed by decomposition of the liquid electrolyte on the surface of the anode will affect  $L$  in eqn (1), we will discuss electrolyte optimization for SIBs with a hard carbon anode.

### 4.1. Sodium storage mechanism in hard carbon

Many researchers have tried to obtain reasonable proof of the sodium storage mechanism. Since the intercalation/nanopore-

filling mechanism<sup>28</sup> was proposed by Stevens and Dahn *et al.* in 2000 as shown in Fig. 3(A), the debate around the mechanism has never stopped. Generally, the primary debate is on the detailed sodiation process during the “sloping part” and “plateau part”, and there are mainly four potential candidates for the two parts of the capacity: defect absorption,<sup>29</sup> nanopore filling,<sup>30</sup> interlayer intercalation,<sup>4</sup> and underpotential deposition.<sup>1</sup> Some typical speculations<sup>3,4,29,31,32</sup> are demonstrated in Fig. 3(B–D) but none of the models can explain all the experimental facts well. For example, considering the influence of the pyrolysis temperature, the absorption–intercalation mechanism seems to gain the upper hand, as higher pyrolysis temperature induces a smaller interlayer distance of nanocrystals of graphite in hard carbon and consequently lowers formation energy for the layer-intercalated  $\text{NaC}_x$  when the distance is less than  $0.47 \text{ nm}$  (most of the hard carbons present an interlayer distance between  $0.37 \text{ nm}$  and  $0.42 \text{ nm}$ ), corresponding to the lower plateau voltage.<sup>4</sup> However, it was reported by Tarascon’s group<sup>33</sup> that no obvious interlayer expansion can be observed using *in situ* XRD detection and the plateau part is mainly nesting in pore-filling, whereas according to the *ab initio* model<sup>34</sup> proposed by Yamada’s group, the sloping and plateau parts of the voltage profile are just the reflection of the energy attenuation for Na-ions being absorbed along the sites (centers of the hexagonal carbon ring) drifting apart from one defect on the graphene layer.

Frankly, it is challenging to prove which storage mechanism is operational, because even the structure of hard carbon still remains uncertain. In 1951, Rosalind Franklin<sup>13</sup> described the non-graphitizing carbon as randomly oriented crystallites with strong cross-linking and offered a vivid 2D schematic (Fig. 4(A)) of the structure. However, hard carbon is not a specific structure but an extensive span of carbonaceous materials, whose structures are extremely complex and are usually correlated closely with the precursors and synthesis process. Structural models<sup>3,30,35,36</sup> on hard carbon are continuously proposed as shown in Fig. 4(B–D). Currently, most of the storage mechanisms are based on the “house of cards” model but whether we can confirm this model is suitable for all hard carbon materials is still in question.



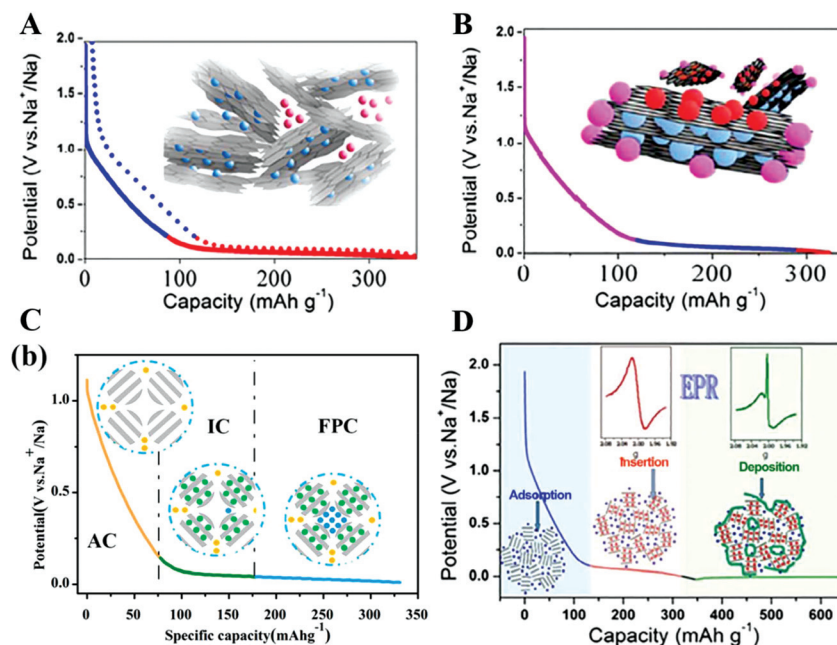


**Fig. 3** The proposed sodium storage mechanism in hard carbon. (A) Visual representation of the "house of cards" model and "intercalation-nano-pore filling" mechanism.<sup>28</sup> Reproduced with permission from ref. 28. Copyright 2015. American Chemical Society. (B) Mechanistic model involving sodium-ion storage at defect sites in the sloping region.<sup>29</sup> Reproduced with permission from ref. 29. Copyright 2015. American Chemical Society. (C) Adsorption-intercalation-pore filling mechanism.<sup>31</sup> Reproduced with permission from ref. 31. Copyright 2018. American Chemical Society. (D) Schematic illustration of the Na ion storage in hard carbons according to the "adsorption-intercalation" mechanism.<sup>3</sup> Reproduced with permission from ref. 3. Copyright 2018. Elsevier.

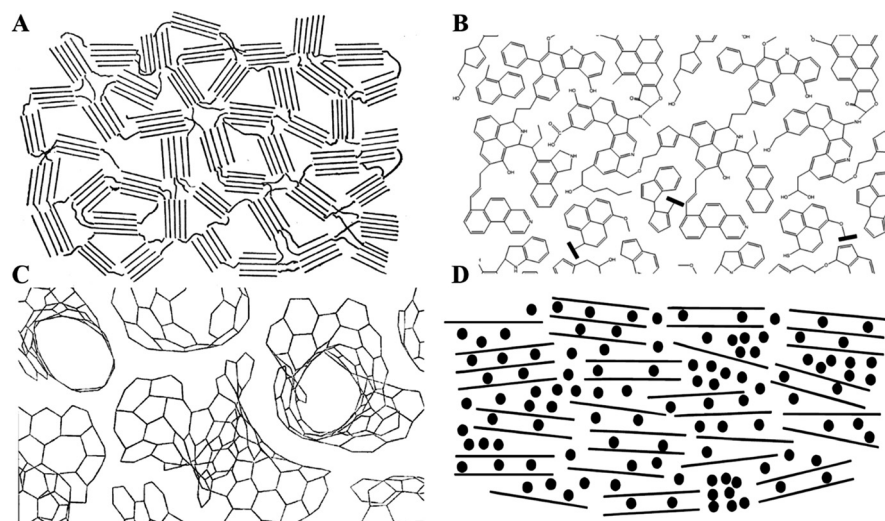


**Fig. 4** The proposed structural model of hard carbon. (A) Proposed by Franklin in 1951.<sup>3,13</sup> Reproduced with permission from ref. 13. Copyright 2018. Elsevier. (B) Proposed by Shinn in 1984.<sup>3,36</sup> Reproduced with permission from ref. 3. Copyright 2018. Elsevier. (C) Proposed by Harris in 1997.<sup>32,35</sup> Reproduced with permission from ref. 32. Copyright 2001. Elsevier. (D) Proposed by Dahn in 2000 (known as the "house of cards" model).<sup>28</sup> Reproduced with permission from ref. 28. Copyright 2000, ECS-The Electrochemical Society.

#### 4.2. Attempts at rational design of hard carbon

While there is debate on the sodium storage mechanism, most researchers agree that the sodium storage mechanism is basically a combination of the 4 possible sodiation processes

mentioned above. Therefore, we can still carry out rational design of high-performance hard carbon to some degree and these attempts will also help to refine the sodium storage mechanism in return. On the road to high-performance hard carbon anodes, much effort<sup>1,8,9,37–39</sup> has been continuously made. Xiao *et al.*<sup>38</sup>



obtained a hard carbon anode with a low defect and low porosity, which delivered a high reversible capacity of  $361 \text{ mA h g}^{-1}$  and an excellent capacity retention of 93.4% after 100 cycles. Lu's group<sup>37</sup> utilized electrospinning to synthesize a phosphorus-functionalized hard carbon anode which exhibited  $393.4 \text{ mA h g}^{-1}$  with the capacity retention up to 98.2% over 100 cycles. Hu and co-workers<sup>9</sup> reported a novel carbon anode derived from charcoal with an ultrahigh high specific capacity of  $\sim 400 \text{ mA h g}^{-1}$ .

Adjusting the micro-structure of hard carbon plays an important role in rational design of hard carbon materials. In general, changing the precursors,<sup>1,40–45</sup> optimizing the pyrolysis process<sup>4,9</sup> and doping heteroatoms<sup>46,47</sup> are the most common and effective methods to modify the microstructure. The hard carbon precursors are mainly derived from a variety of organics or biomass,<sup>3,40</sup> such as banana peels,<sup>44</sup> tea leaves,<sup>45</sup> cellulose<sup>41</sup> and even cotton,<sup>43</sup> and the different precursors usually exhibit different chemical components and microstructures and consequently result in hard carbon with different nano- and micro-structures. The cost of raw materials and yield should also be taken into consideration. Li *et al.*<sup>48</sup> obtained a HC anode from the cheap anthracite in an environmentally friendly way and the yield is as high as 90%, which is now being industrialized for its low cost. The pyrolysis process is also important for tuning the microstructure. By modifying the pyrolysis process, Zhao *et al.*<sup>9</sup> developed a hard carbon with a specific capacity of  $\sim 400 \text{ mA h g}^{-1}$ , and 85% of its capacity was provided by the plateau part. It is also reported that the higher pyrolysis temperature may also lead to a smaller Brunauer–Emmett–Teller (BET) surface area and consequently a higher ICE.<sup>1,9,49</sup> Note that in the context of the *p* evaluation of the full-cell, ICE is as important as the specific capacity of hard carbon, as both of them impact *C/E* of the full-cell, and evaluation of one newly designed hard carbon needs to focus on *p*, not just specific capacity.

As for heteroatom doping, the mechanism is quite complex because the outcome highly depends on the dopant type and a commonly accepted sodium storage mechanism picture is still absent even for pure hard carbon itself. It was reported that certain doping such as S<sup>50</sup> and P<sup>46</sup> will introduce more carbon defects, which will increase the sloping capacity. Also, it is reported that with P as the dopant, the formation of P=O and P–C bonds in the nano-graphitic layer will increase the capacity.<sup>37</sup> One aspect to note is that if the dopant is selected without well-rounded considerations from the practical full-cell perspective, SIBs may exhibit a totally opposite change in behavior such as lower plateau capacity.<sup>46</sup> It is also worth mentioning again that heteroatom doping usually brings a lower ICE compared to the original hard carbon,<sup>38</sup> which may sometimes bring a Pyrrhic victory and cause higher *C/E* of the full-cell.<sup>46</sup> Therefore, researchers have to evaluate the practicability of heteroatom doping under the consideration of *p*.

#### 4.3. Electrolyte optimization for SIBs with a hard carbon anode

Electrolytes are hugely important for the total price and cyclability of the battery, further affecting the *L* and *p* value.<sup>51</sup>

Here, we will review choosing appropriate electrolytes for hard carbon from the full-cell perspective.

First, more effort should be paid to NaPF<sub>6</sub>-based or NaFSI/NaTFSI-based electrolytes rather than NaClO<sub>4</sub>-based electrolytes since NaClO<sub>4</sub> could easily cause explosion.<sup>51</sup> The salt concentration should be carefully tuned because the higher concentration may bring anion-derived stable SEIs, at the cost of increasing the price and electrolyte viscosity.<sup>52</sup> How to balance the relationship between these issues should fully consider the full-cell perspective mentioned above. It is wise to compromise and develop a moderately concentrated electrolyte, and it is reported that an appropriate salt concentration of electrolyte,<sup>53,54</sup> for example, 3 M NaFSI in PC:EC, can also improve the flame-retardant properties, which are important for industrial applications. Besides, an appropriate electrolyte content in SIBs should be taken into consideration. For graphite//NMC532 LIBs, it is reported that the minimum injected electrolyte (1.2 M LiPF<sub>6</sub> in EC:EMC) volume is about 1.9 times the total pore volume in the anode, cathode and separator to guarantee decent performance of full-cells, including long cyclability and acceptable ohmic resistance.<sup>55</sup> However, relevant research studies in SIBs are still largely absent, and seeking an appropriate electrolyte volume based on the full-cell metric in SIBs with hard carbon should be carried out expeditiously.

Second, to improve the cycle life of SIBs, the electrolyte should be essential for forming contiguous and stable SEI, which is closely related to solvents, additives, salt concentration and binder. Solvent is usually made of polar molecules like EC or PC to achieve high solubility for salts, with chain molecules like DMC or DEC for viscosity reduction. It is worth mentioning that EC is essential in graphite-based LIBs because it can help in forming stable SEIs.<sup>56</sup> In contrast, the relatively higher absolute potential of hard carbon in SIBs at the end of the charging process may prevent EC or other esters from forming a stable organic layer.<sup>57,58</sup> Instead, long-neglected ether-based electrolytes<sup>56,59–62</sup> in LIBs are continuously reported to exhibit excellent properties when pairing hard carbon with Na<sub>BCC</sub> metal counter, such as the long cycle life,<sup>61</sup> high capacity,<sup>60</sup> and excellent rate performance.<sup>62</sup> However, whether these improvements can reemerge in practical full-cells without the Na<sub>BCC</sub> metal counter still remains questionable (especially with regard to high-voltage stability on the cathode side) and only further investigations can tell which kind of solvent is more suitable for practical full-cell SIBs with a hard carbon anode. The experience of solvent selection for both esters and ethers in LIBs should be reconsidered due to the difference between SIBs and LIBs.

Another currently urgent issue is that most of the investigations on electrolyte optimization for SIBs are carried out in a half-cell system and the conclusion might be unsuitable for the sodium-matched full-cell, due to the huge difference between the Na<sub>BCC</sub>-metal counter electrode and a real cathode<sup>51,57,63,64</sup> as discussed previously. FEC and other additives must be reconsidered for their compatibility with the hard carbon anode in well matched full-cell SIBs. Meanwhile, it is worth mentioning that the binder can assist in forming a





protective layer on the electrode and reducing the continuous growth of SEI,<sup>65</sup> which was usually overlooked in previous studies.

## 5. Summary

SIBs were developed not much later than LIBs, but the investigation did not gain enough traction until the last decade or so. In this review, a full-cell perspective is offered and then some often-ignored issues such as the CE-cycle life relation and underestimated reversible capacity results are presented to encourage the researchers to be careful about SIB half-cell test results, due to the extraordinary reactivity and excessive impedance brought by the Na<sub>BCC</sub> metal counter-electrode, which is much more extreme than the Li<sub>BCC</sub> metal counter-electrode. A revised half-cell test method that can measure ICE and real capacity of hard carbon more precisely is introduced to lay the foundation for full-cell design. The full-cell configuration is always recommended to assess the true cycle life, due to the soluble redox mediators brought by the reaction of Na<sub>BCC</sub> with the electrolyte, which can cause the half-cell CE to be overly pessimistic in predicting the full-cell cycle life. Transition-metal oxide cathodes such as Na[Cu<sub>1/9</sub>Ni<sub>2/9</sub>Fe<sub>1/3</sub>Mn<sub>1/3</sub>]O<sub>2</sub> are suggested to be the promising configuration, for both the investigations of the hard carbon anode and the electrolyte, and moderately concentrated electrolytes such as 3 M NaFSI in PC:EC are recommended. After clarifying these basic issues, we further probe into rational design of hard carbon materials and electrolytes from the full-cell perspective. There is a high chance that the hard carbon anode will be dominant in SIBs and become the first to enter the arena competing with LIBs.

## Conflicts of interest

The authors declare no conflict of interest.

## Acknowledgements

The authors are grateful for the support from Tongji University and the National Natural Science Foundation of China (NSFC-No. 51602222 and 51632001). JL acknowledges support of NSF ECCS-1610806.

## References

- 1 Y. Zheng, Y. Wang, Y. Lu, Y.-S. Hu and J. Li, A high-performance sodium-ion battery enhanced by macadamia shell derived hard carbon anode, *Nano Energy*, 2017, **39**, 489–498.
- 2 N. Sun, H. Liu and B. Xu, Facile synthesis of high performance hard carbon anode materials for sodium ion batteries, *J. Mater. Chem. A*, 2015, **3**(41), 20560–20566.
- 3 X. Dou, I. Hasa, D. Saurel, C. Vaalma, L. Wu, D. Buchholz, *et al.*, Hard carbons for sodium-ion batteries: Structure, analysis, sustainability, and electrochemistry, *Mater. Today*, 2019, **23**, 87–104.
- 4 S. Qiu, L. Xiao, M. L. Sushko, K. S. Han, Y. Shao, M. Yan, *et al.*, Manipulating Adsorption-Insertion Mechanisms in Nanostructured Carbon Materials for High-Efficiency Sodium Ion Storage, *Adv. Energy Mater.*, 2017, **7**(17), 1700403.
- 5 P.-F. Wang, Y. You, Y.-X. Yin and Y.-G. Guo, Layered Oxide Cathodes for Sodium-Ion Batteries: Phase Transition, Air Stability, and Performance, *Adv. Energy Mater.*, 2018, **8**(8), 1701912.
- 6 P. Barpanda, L. Lander, S.-I. Nishimura and A. Yamada, Polyanionic Insertion Materials for Sodium-Ion Batteries, *Adv. Energy Mater.*, 2018, **8**(17), 1703055.
- 7 H. Guo, Y. Wang, W. Han, Z. Yu, X. Qi, K. Sun, *et al.*, Na-deficient O3-type cathode material Na<sub>0.8</sub>[Ni<sub>0.3</sub>Co<sub>0.2</sub>Ti<sub>0.5</sub>]O<sub>2</sub> for room-temperature sodium-ion batteries, *Electrochim. Acta*, 2015, **158**, 258–263.
- 8 Y. Zheng, Y. Lu, X. Qi, Y. Wang, L. Mu, Y. Li, *et al.*, Superior electrochemical performance of sodium-ion full-cell using poplar wood derived hard carbon anode, *Energy Storage Mater.*, 2019, **18**, 269–279.
- 9 C. Zhao, Q. Wang, Y. Lu, B. Li, L. Chen and Y.-S. Hu, High-temperature treatment induced carbon anode with ultra-high Na storage capacity at low-voltage plateau, *Sci. Bull.*, 2018, **63**(17), 1125–1129.
- 10 E. J. Berg, C. Villevieille, D. Streich, S. Trabesinger and P. Novák, Rechargeable Batteries: Grasping for the Limits of Chemistry, *J. Electrochem. Soc.*, 2015, **162**(14), A2468–A2475.
- 11 Z. Li, Z. Jian, X. Wang, I. A. Rodriguez-Perez, C. Bommier and X. Ji, Hard carbon anodes of sodium-ion batteries: undervalued rate capability, *Chem. Commun.*, 2017, **53**(17), 2610–2613.
- 12 Y. Qi, Y. Lu, F. Ding, Q. Zhang, H. Li, X. Huang, *et al.*, Slope-Dominated Carbon Anode with High Specific Capacity and Superior Rate Capability for High Safety Na-Ion Batteries, *Angew. Chem., Int. Ed.*, 2019, **58**(13), 4361–4365.
- 13 R. E. Franklin, Crystallite growth in graphitizing and non-graphitizing carbons, *Proc. R. Soc. A*, 1951, **209**(1097), 196.
- 14 K. Kamiya, M. Inagaki and T. Noda, Microscopic observations of hard carbon heat-treated under pressure, *Carbon*, 1971, **9**(3), 287–289.
- 15 C. Yokokawa, K. Hosokawa and Y. Takegami, Low temperature catalytic graphitization of hard carbon, *Carbon*, 1966, **4**(4), 459–465.
- 16 C. Yokokawa, K. Hosokawa and Y. Takegami, A kinetic study of catalytic graphitization of hard carbon, *Carbon*, 1967, **5**(5), 475–480.
- 17 L. Mu, S. Xu, Y. Li, Y. S. Hu, H. Li, L. Chen, *et al.*, Prototype Sodium-Ion Batteries Using an Air-Stable and Co/Ni-Free O3-Layered Metal Oxide Cathode, *Adv. Mater.*, 2015, **27**(43), 6928–6933.





- 18 G. Yan, S. Mariyappan, G. Rousse, Q. Jacquet, M. Deschamps, R. David, *et al.*, Higher energy and safer sodium ion batteries via an electrochemically made disordered Na<sub>3</sub>V<sub>2</sub>(PO<sub>4</sub>)<sub>2</sub>F<sub>3</sub> material, *Nat. Commun.*, 2019, **10**(1), 585.
- 19 W. Xue, L. Miao, L. Qie, C. Wang, S. Li, J. Wang, *et al.*, Gravimetric and volumetric energy densities of lithium-sulfur batteries, *Curr. Opin. Electrochem.*, 2017, **6**(1), 92–99.
- 20 J. Wang, P. Liu, J. Hicks-Garner, E. Sherman, S. Soukiazian, M. Verbrugge, *et al.*, Cycle-life model for graphite-LiFePO<sub>4</sub> cells, *J. Power Sources*, 2011, **196**(8), 3942–3948.
- 21 J. Wang, J. Purewal, P. Liu, J. Hicks-Garner, S. Soukiazian, E. Sherman, *et al.*, Degradation of lithium ion batteries employing graphite negatives and nickel-cobalt-manganese oxide + spinel manganese oxide positives: Part 1, aging mechanisms and life estimation, *J. Power Sources*, 2014, **269**, 937–948.
- 22 A. J. Smith, J. C. Burns, S. Trussler and J. R. Dahn, Precision Measurements of the Coulombic Efficiency of Lithium-Ion Batteries and of Electrode Materials for Lithium-Ion Batteries, *J. Electrochem. Soc.*, 2010, **157**(2), A196.
- 23 Y. Jin, S. Li, A. Kushima, X. Zheng, Y. Sun, J. Xie, *et al.*, Self-healing SEI enables full-cell cycling of a silicon-majority anode with a coulombic efficiency exceeding 99.9%, *Energy Environ. Sci.*, 2017, **10**(2), 580–592.
- 24 S. E. Sloop, J. B. Kerr and K. Kinoshita, The role of Li-ion battery electrolyte reactivity in performance decline and self-discharge, *J. Power Sources*, 2003, **119–121**, 330–337.
- 25 D. I. Iermakova, R. Dugas, M. R. Palacin and A. Ponrouch, On the Comparative Stability of Li and Na Metal Anode Interfaces in Conventional Alkyl Carbonate Electrolytes, *J. Electrochem. Soc.*, 2015, **162**(13), A7060–A7066.
- 26 J. Conder and C. Villevieille, How reliable is the Na metal as a counter electrode in Na-ion half cells?, *Chem. Commun.*, 2019, **55**(9), 1275–1278.
- 27 K. Yan, Z. Lu, H.-W. Lee, F. Xiong, P.-C. Hsu, Y. Li, *et al.*, Selective deposition and stable encapsulation of lithium through heterogeneous seeded growth, *Nat. Energy*, 2016, **1**, 16010.
- 28 D. A. Stevens and J. R. Dahn, High capacity anode materials for rechargeable sodium-ion batteries, *J. Electrochem. Soc.*, 2000, **147**(4), 1271–1273.
- 29 C. Bommier, T. W. Surta, M. Dolgos and X. Ji, New Mechanistic Insights on Na-Ion Storage in Nongraphitizable Carbon, *Nano Lett.*, 2015, **15**(9), 5888–5892.
- 30 D. A. Steven and J. R. Dahn, An In Situ Small-Angle X-Ray Scattering Study of Sodium Insertion into a Nanoporous Carbon Anode Material within an Operating Electrochemical Cell, *J. Electrochem. Soc.*, 2000, **147**(12), 4428–4431.
- 31 Y. Jin, S. Sun, M. Ou, Y. Liu, C. Fan, X. Sun, *et al.*, High-Performance Hard Carbon Anode: Tunable Local Structures and Sodium Storage Mechanism, *ACS Appl. Energy Mater.*, 2018, **1**(5), 2295–2305.
- 32 P. J. F. Harris, Non-graphitizing Carbons, in *Encyclopedia of Materials: Science and Technology*, ed. K. H. J. Buschow, R. W. Cahn, M. C. Flemings, B. Ilschner, E. J. Kramer and S. Mahajan, *et al.*, Elsevier, Oxford, 2001, pp. 6197–6202.
- 33 B. Zhang, C. M. Ghimbeu, C. Laberty, C. Vix-Guterl and J.-M. Tarascon, Correlation Between Microstructure and Na Storage Behavior in Hard Carbon, *Adv. Energy Mater.*, 2016, **6**(1), 1501588.
- 34 P.-C. Tsai, S.-C. Chung, S.-K. Lin and A. Yamada, Ab initio study of sodium intercalation into disordered carbon, *J. Mater. Chem. A*, 2015, **3**(18), 9763–9768.
- 35 P. J. F. Harris and S. C. Tsang, High-resolution electron microscopy studies of non-graphitizing carbons, *Philos. Mag. A*, 1997, **76**(3), 667–677.
- 36 J. H. Shinn, From Coal to Single-Stage and 2-Stage Products - a Reactive Model of Coal Structure, *Fuel*, 1984, **63**(9), 1187–1196.
- 37 Y. Li, Y. Yuan, Y. Bai, Y. Liu, Z. Wang, L. Li, *et al.*, Insights into the Na + Storage Mechanism of Phosphorus-Functionalized Hard Carbon as Ultrahigh Capacity Anodes, *Adv. Energy Mater.*, 2018, **8**(18), 1702781.
- 38 L. Xiao, H. Lu, Y. Fang, M. L. Sushko, Y. Cao, X. Ai, *et al.*, Low-Defect and Low-Porosity Hard Carbon with High Coulombic Efficiency and High Capacity for Practical Sodium Ion Battery Anode, *Adv. Energy Mater.*, 2018, **8**(20), 1703238.
- 39 Y. Wang, Z. Feng, W. Zhu, V. Garipey, C. Gagnon, M. Provencher, *et al.*, High Capacity and High Efficiency Maple Tree-Biomass-Derived Hard Carbon as an Anode Material for Sodium-Ion Batteries, *Materials*, 2018, **11**(8), 1294.
- 40 Y. Li, S. Xu, X. Wu, J. Yu, Y. Wang, Y.-S. Hu, *et al.*, Amorphous monodispersed hard carbon micro-spherules derived from biomass as a high performance negative electrode material for sodium-ion batteries, *J. Mater. Chem. A*, 2015, **3**(1), 71–77.
- 41 V. Simone, A. Boulineau, A. de Geyer, D. Rouchon, L. Simonin and S. Martinet, Hard carbon derived from cellulose as anode for sodium ion batteries: Dependence of electrochemical properties on structure, *J. Energy Chem.*, 2016, **25**(5), 761–768.
- 42 Y.-X. Wang, S.-L. Chou, J. H. Kim, H.-K. Liu and S.-X. Dou, Nanocomposites of silicon and carbon derived from coal tar pitch: Cheap anode materials for lithium-ion batteries with long cycle life and enhanced capacity, *Electrochim. Acta*, 2013, **93**, 213–221.
- 43 Y. Li, Y.-S. Hu, M.-M. Titirici, L. Chen and X. Huang, Hard Carbon Microtubes Made from Renewable Cotton as High-Performance Anode Material for Sodium-Ion Batteries, *Adv. Energy Mater.*, 2016, **6**(18), 1600659.
- 44 E. M. Lotfabad, J. Ding, K. Cui, A. Kohandehghan, W. P. Kalisvaart, M. Hazelton and D. Mitlin, High-Density Sodium and Lithium Ion Battery Anodes from Banana Peels, *ACS Nano*, 2014, **8**, 7115–7129.
- 45 A. A. Arie, B. Tekin, E. Demir and R. Demir-Cakan, Utilization of The Indonesian's Spent Tea Leaves as Promising Porous Hard Carbon Precursors for Anode



- Materials in Sodium Ion Batteries, *Waste Biomass Valorization*, 2019, DOI: 10.1007/s12649-019-00624-x.
- 46 Z. Li, C. Bommier, Z. S. Chong, Z. Jian, T. W. Surta, X. Wang, *et al.*, Mechanism of Na-Ion Storage in Hard Carbon Anodes Revealed by Heteroatom Doping, *Adv. Energy Mater.*, 2017, 7(18), 1602894.
  - 47 K. C. Wasalathilake, G. A. Ayoko and C. Yan, Effects of heteroatom doping on the performance of graphene in sodium-ion batteries: A density functional theory investigation, *Carbon*, 2018, 140, 276–285.
  - 48 Y. Li, Y.-S. Hu, X. Qi, X. Rong, H. Li, X. Huang, *et al.*, Advanced sodium-ion batteries using superior low cost pyrolyzed anthracite anode: towards practical applications, *Energy Storage Mater.*, 2016, 5, 191–197.
  - 49 C. Matei Ghimbeu, J. Górka, V. Simone, L. Simonin, S. Martinet and C. Vix-Guterl, Insights on the Na + ion storage mechanism in hard carbon: Discrimination between the porosity, surface functional groups and defects, *Nano Energy*, 2018, 44, 327–335.
  - 50 L. Qie, W. Chen, X. Xiong, C. Hu, F. Zou, P. Hu, *et al.*, Sulfur-Doped Carbon with Enlarged Interlayer Distance as a High-Performance Anode Material for Sodium-Ion Batteries, *Adv. Sci.*, 2015, 2(12), 1500195.
  - 51 Y. Huang, L. Zhao, L. Li, M. Xie, F. Wu and R. Chen, Electrolytes and Electrolyte/Electrode Interfaces in Sodium-Ion Batteries: From Scientific Research to Practical Application, *Adv. Mater.*, 2019, 31(21), 1808393.
  - 52 K. Takada, Y. Yamada, E. Watanabe, J. Wang, K. Sodeyama, Y. Tateyama, *et al.*, Unusual Passivation Ability of Superconcentrated Electrolytes toward Hard Carbon Negative Electrodes in Sodium-Ion Batteries, *ACS Appl. Mater. Interfaces*, 2017, 9(39), 33802–33809.
  - 53 J. Patra, H.-T. Huang, W. Xue, C. Wang, A. S. Helal, J. Li and J.-K. Chang, Moderately concentrated electrolyte improves solid-electrolyte interphase and sodium storage performance of hard carbon, *Energy Storage Mater.*, 2019, 16, 146–154.
  - 54 X. Liu, X. Jiang, Z. Zeng, X. Ai, H. Yang, F. Zhong, *et al.*, High Capacity and Cycle-Stable Hard Carbon Anode for Nonflammable Sodium-Ion Batteries, *ACS Appl. Mater. Interfaces*, 2018, 10(44), 38141–38150.
  - 55 S. J. An, J. Li, D. Mohanty, C. Daniel, B. J. Polzin, J. R. Croy, *et al.*, Correlation of Electrolyte Volume and Electrochemical Performance in Lithium-Ion Pouch Cells with Graphite Anodes and NMC532 Cathodes, *J. Electrochem. Soc.*, 2017, 164(6), A1195–A1202.
  - 56 B. Xiao, T. Rojo and X. Li, Hard Carbon as Sodium-Ion Battery Anodes: Progress and Challenges, *ChemSusChem*, 2019, 12(1), 133–144.
  - 57 S. Komaba, W. Murata, T. Ishikawa, N. Yabuuchi, T. Ozeki, T. Nakayama, *et al.*, Electrochemical Na Insertion and Solid Electrolyte Interphase for Hard-Carbon Electrodes and Application to Na-Ion Batteries, *Adv. Funct. Mater.*, 2011, 21(20), 3859–3867.
  - 58 B. Philippe, M. Valvo, F. Lindgren, H. Rensmo and K. Edström, Investigation of the Electrode/Electrolyte Interface of Fe<sub>2</sub>O<sub>3</sub> Composite Electrodes: Li vs Na Batteries, *Chem. Mater.*, 2014, 26(17), 5028–5041.
  - 59 J. Zhang, D.-W. Wang, W. Lv, L. Qin, S. Niu, S. Zhang, *et al.*, Ethers Illuminate Sodium-Based Battery Chemistry: Uniqueness, Surprise, and Challenges, *Adv. Energy Mater.*, 2018, 8(26), 1801361.
  - 60 J. Zhang, D.-W. Wang, W. Lv, S. Zhang, Q. Liang, D. Zheng, *et al.*, Achieving superb sodium storage performance on carbon anodes through an ether-derived solid electrolyte interphase, *Energy Environ. Sci.*, 2017, 10(1), 370–376.
  - 61 P. Bai, Y. He, P. Xiong, X. Zhao, K. Xu and Y. Xu, Long cycle life and high rate sodium-ion chemistry for hard carbon anodes, *Energy Storage Mater.*, 2018, 13, 274–282.
  - 62 Y.-E. Zhu, L. Yang, X. Zhou, F. Li, J. Wei and Z. Zhou, Boosting the rate capability of hard carbon with an ether-based electrolyte for sodium ion batteries, *J. Mater. Chem. A*, 2017, 5(20), 9528–9532.
  - 63 Y. B. Niu, Y. X. Yin and Y. G. Guo, Nonaqueous Sodium-Ion Full Cells: Status, Strategies, and Prospects, *Small*, 2019, 15(32), e1900233.
  - 64 J. Tang, J. Barker and V. G. Pol, Sodium-Ion Battery Anodes Comprising Carbon Sheets: Stable Cycling in Half- and Full-Pouch Cell Configuration, *Energy Technol.*, 2018, 6(1), 213–220.
  - 65 J. Patra, P. C. Rath, C. Li, H. M. Kao, F. M. Wang, J. Li, *et al.*, A Water-Soluble NaCMC/NaPAA Binder for Exceptional Improvement of Sodium-Ion Batteries with an SnO<sub>2</sub>-Ordered Mesoporous Carbon Anode, *ChemSusChem*, 2018, 11(22), 3923–3931.

